Original Article

CLINICAL AND EXPERIMENTAL VACCINE RESEARCH

Clin Exp Vaccine Res. 2025 Jan;14(1):23-34
https://doi.org/10.7774/cevr.2025.14.e7
pISSN 2287-3651·eISSN 2287-366X

# Immunogenicity and protection of recombinant self-assembling ferritin-hemagglutinin nanoparticle influenza vaccine in mice

**Xu Wang [1], Ziyao Qin [1], Min Zhang [1], Baoyuan Shang [1], Zhilei Li [1], Meiyi Zhao [1], Qing Tang [1], Qi Tang [1], Jian Luo [1,2]**

[1]Department of Virology & Vaccine, Shanghai Institute of Biological Products, Shanghai, China
[2]State Key Laboratory of Novel Vaccines for Emerging Infectious Diseases, Beijing, China

OPEN ACCESS

Received: Dec 1, 2024
Revised: Dec 21, 2024
Accepted: Dec 21, 2024
Published online: Jan 17, 2025

Corresponding author:
Jian Luo, PhD
Department of Virology & Vaccine, Shanghai Institute of Biological Products, No. 350 Anshun Road, Shanghai 200051, China.
Tel: +86-021-62750096
Fax: +86-021-62834337
Email: rojjer2009@hotmail.com

**Purpose:** Influenza virus remains a serious burden to global public health. Current influenza vaccine fails to provide impeccable protection efficacy to the annual seasonal influenza and cannot offer a timely response to potential pandemic influenza. It is necessary to develop next generation influenza vaccines to solve the current dilemma.
**Materials and Methods:** We developed a recombinant, self-assembling ferritin nanoparticle that presents the extracellular domain of the influenza hemagglutinin antigen on its surface, designated as ferritin-HA. After characterizing its structure and properties, we evaluated its capacity to trigger an immune response and offer protection against influenza virus challenge in a mouse model.
**Results:** The recombinant ferritin-HA protein expressed in Chinese hamster ovary cells assembles into nanoparticles of a defined size. This nanoparticle vaccine enhances the uptake efficiency of Dendritic cells and promotes their maturation. Immunization with ferritin-HA nanoparticle in mice induced high levels of immunoglobulin G, hemagglutination inhibition antibodies, and microneutralization antibodies, demonstrating their stronger immunogenicity compared to current split virion vaccines. Additionally, ferritin-HA nanoparticle conferred well protection against a lethal challenge with a heterologous H3N2 influenza virus in mice.
**Conclusion:** This study indicates that a self-assembling ferritin-HA nanoparticle has great potential for enhancing immune response and protective efficacy in mice, presenting a promising strategy for developing next generation influenza vaccine candidate.

**Keywords:** Influenza; Ferritin; Nanovaccine; Humoral immunity

## INTRODUCTION

Influenza, a severe acute respiratory disease, is caused by the influenza virus and affects 5%–15% of the global population, causing up to 650,000 deaths annually [1-3]. Vaccination is the most effective way to prevent seasonal and pandemic influenza caused by influenza viruses. However, the overall effectiveness of currently approved influenza vaccines ranges from 40% to 60% due to several reasons [4], including the mismatch between circulating strains and vaccine strains, rapid antigen drift

(especially in the H3N2 virus), and adaptive mutations during vaccine production in chicken embryo [5-9].

Recombinant protein vaccine technology circumvents the adaptive mutations that occur in chicken embryos, enabling rapid and precise expression of key viral antigens. Nanoparticle vaccines represent a crucial category of recombinant protein vaccines, with ferritin emerging as a promising carrier for vaccine delivery in recent years. Ferritin can self-assemble into nanoparticles that present antigens on their surface and deliver antigens or drugs within their inner cavities. Furthermore, its excellent biocompatibility, biodegradability, stability, and surface modifiability make ferritin an ideal candidate for vaccine development [10].

Ferritin-based recombinant nanoparticle vaccines have been utilized in the development of various vaccines, including those for Epstein-Barr virus [11], human immunodeficiency virus [12], respiratory syncytial virus [13], and severe acute respiratory syndrome coronavirus 2 [14,15]. The candidate influenza vaccine H1ssF, using ferritin to display the hemagglutinin (HA) stem region, has completed phase 1 clinical trials with positive results, indicating the potential of the ferritin platform in influenza vaccine development [16,17].

In this study, we designed an influenza nanoparticle vaccine candidate based on a self-assembling ferritin derived from the non-heme ferritin of *Helicobacter pylori*. Using the self-assembling properties and unique spatial site resistance of ferritin, we displayed the extracellular domain of the HA from influenza virus A/Darwin/9/2021 (H3N2) on its surface. HA was inserted at the interface of adjacent subunits so that it spontaneously assembles and generates eight trimeric HA on its surface. Meanwhile, we aimed to determine the immune responses and its protective effect in mice. The results demonstrated that ferritin-HA elicited a strong humoral response, producing higher levels of virus specific immunoglobulin G (IgG), hemagglutination inhibition (HI) antibodies, and microneutralization (MN) antibodies compared to the monovalent split virion influenza vaccine. Additionally, it induced neutralizing antibodies against the virus of A/Guizhou/54/1989 (H3N2) and provided partial protection to mice against this virus.

## MATERIALS AND METHODS

### Cells, vaccines, proteins and viruses

ExpiCHO-S cells were cultured in serum-free medium (ExpiCHO Expression Medium; Gibco, Waltham, MA, USA), while Madin-Darby Canine Kidney (MDCK) cells were cultured in complete Dulbecco's Modified Eagle's Medium (DMEM; Gibco) with 10% fetal bovine serum (Gibco). JAWS II cells were cultured in Minimum Essential Medium-α (JAWS II Specialized Medium; Saios Chemical Instrument Co., Ltd., Wuhan, China) supplemented with 20% fetal bovine serum, 5 ng/mL murine granulocyte macrophage-colony stimulating factor, and 1% glutamine.

The egg-based monovalent influenza split virion vaccine (MIV) of A/Darwin/9/2021 (H3N2) virus strain was prepared by the Shanghai Institute of Biological Products (Shanghai, China).

Recombinant ferritin (Zhongsheng Biologicals, Beijing, China) was used as a control for mouse immunization.

The mouse-adapted influenza virus A/Guizhou/54/1989 (H3N2) used for the challenge study was amplified in 8–10 days old specific pathogen free (SPF) chicken embryos, then sub-packed and stored at –80°C.

### Design and production of recombinant ferritin-HA protein

Based on the codon preferences of CHO cells, we optimized and synthesized the gene sequence encoding the ferritin-HA DNA (GenScript, Nanjing, China) (extracellular segment of HA [1-529] from A/Darwin/9/2021 [H3N2] virus; GenBank: WND60806.1) and inserted it into the expression plasmid pcDNA3.4. To stabilize the HA conformation, amino acid residues at the HA1 and HA2 junction were modified (P340A, E350A, Q352S, T353S, R354A) [18]. The ferritin comprised residues 5-167 (GenBank: NP_223316) and introduced a point mutation (N19Q) to eliminate potential N-linked glycosylation sites. A flexible linker (Ser-Gly-Gly) was used to connect the C-terminus of HA and the N-terminus of ferritin. Eight repeated histidine tags were appended after the HA signal peptide (1-16) to facilitate protein purification.

The expression vector was transfected into ExpiCHO-S cells using ExpiFectamine (Gibco), and the supernatant was collected after 10 days of culture. Nanoparticles were purified through nickel affinity chromatography (GE Healthcare, Chicago, IL, USA) and dialyzed overnight in phosphate-buffered saline (PBS; pH 7.4). The purified protein was verified by Western blot using a mouse anti-His tag antibody (Merck, Carrigtwohill, Ireland), with chemiluminescent detection performed on Hyperfilm™ ECL™ film (Cytiva, Marlborough, MA, USA) and imaged using the Azure Imaging System (Azure Biosystems, Dublin, CA, USA). The protein was concentrated using 100 kDa ultrafiltration tubes (Amicon Ultra; Merck), and its concentration was measured by the BCA method (Thermo Fisher Scientific, Waltham, MA, USA). The purified protein was then sterilized by filtration, aliquoted, and stored at –80°C.

### Characterization of recombinant ferritin-HA protein

To characterize the morphology of the nanoparticles, we

 https://doi.org/10.7774/cevr.2025.14.e7

used dynamic light scattering with a Zetasizer Nano ZS (Malvern Instruments, Malvern, UK) to determine their size. Transmission electron microscopy (TEM; JEOL Ltd., Akishima, Japan) was employed to capture images and confirm the protein's actual structure. The oligomeric ratio and purity of the ferritin-HA were analyzed via High Performance Liquid Chromatography (HPLC), using a Zenix-C SEC-150 column (Sepax Technologies, Suzhou, China) on an Agilent 1260 Infinity II system (Agilent Technologies, Santa Clara, CA, USA).

### Visualization of antigen uptaking and maturation of dendritic cells (DCs)

To assess the uptake of ferritin-HA and MIV by DCs, JAWS II cells (mouse bone marrow-derived immature DCs) were seeded at a density of $1\times10^5$ cells/well in 12-well plates and cultured at 37°C for 24 hours. Equal amounts of Alexa Fluor 488-labeled MIV and ferritin-HA (Abcam, Cambridge, MA, USA) were added and incubated at 37°C for another 24 hours. Cells were washed twice with PBS and imaged by a confocal microscope (IXplore SpinSR, Olympus, Japan).

To assess the ability of ferritin-HA and MIV to induce DCs maturation, JAWS II cells were seeded at a density of $1\times10^5$ cells/well in 24-well plates. After 24 hours of culture, 50 μg of ferritin-HA or MIV was added to the wells and co-cultured for 36 hours. Cells were collected and stained for CD80, and flow cytometry was performed using the Attune NxT Acoustic Focusing Cytometer (Invitrogen, Waltham, MA, USA).

### Vaccination and challenge

SPF female BALB/c mice, aged 4 to 6 weeks, were purchased from Zhejiang Vital River Laboratory Animal Technology Co., Ltd. (Beijing, China). The animal experimental protocol (protocol number: 2023006) was approved by the Animal Management Committee and the Animal Ethics and Welfare Protection Group of the Shanghai Institute of Biological Products. All animal experiments adhered to the animal ethics guidelines of the National Health and Medical Research Council of China.

For the immunogenicity study, 4 to 6-week-old BALB/c mice were intramuscularly injected twice with the ferritin-HA nanoparticle vaccine at 21-day intervals, with HA doses of 0.15, 0.015, or 0.015 μg combined with 0.5 mg/mL aluminum hydroxide ($Al[OH]_3$; Life Science, Nanjing, China). Another group received an injection of MIV containing 0.15 μg HA. The PBS group and the 0.15 μg ferritin group served as control groups. Blood samples were collected on day 21 and 42 and stored at –20°C for subsequent serological analysis.

For the challenge study, immunized BALB/c mice were challenged with $5\times LD_{50}$ of the A/Guizhou/54/1989 (H3N2) virus on day 28 post the final immunization. The clinical signs of the mice were monitored daily, and their body weights were recorded each day. Five days post-challenge, the right lung of each mouse was harvested for homogenization (**Fig. 1**). The infectious virus in the lung homogenates was determined by the 50% tissue culture infectious dose ($TCID_{50}$) assay with MDCK cells, as described previously [19].

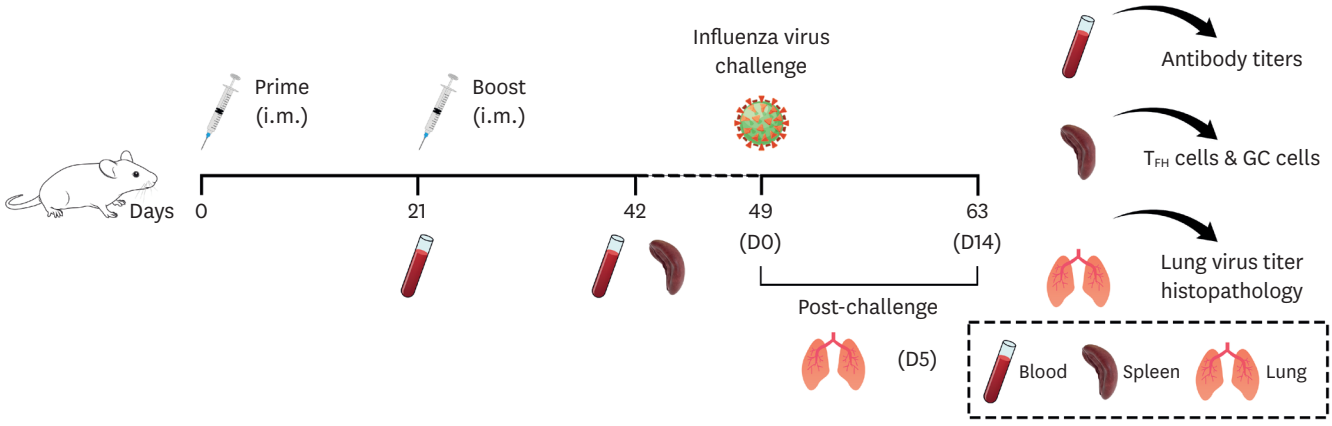


**Fig. 1.** Schematic of the immunization, virus challenge and sampling strategy. BALB/c mice received intramuscular injections of the ferritin-HA vaccine following a primary-boost immunization protocol, followed by viral challenge and tissue sampling. Blood samples were collected from the tail vein on day 21 post both the prime and boost immunization, with spleen samples collected on day 21 post boost immunization. On day 28 post boost immunization, mice were challenged with a lethal dose ($5\times LD_{50}$) of A/Guizhou/54/1989 (H3N2) virus. Body weight and survival were monitored for 14 days post-challenge. Lung tissue samples were collected on day 5 post challenge and analyzed for residual viral load and pathological changes.
HA, hemagglutinin; $T_{FH}$, follicular helper T; GC, germinal center.

### Enzyme-linked immunosorbent assay (ELISA)

MIV or trimeric HA protein (Sino Biological, Beijing, China) was coated onto high-binding clear flat-bottom 96-well plates at 500 ng/well and incubated overnight at 4°C. Mouse sera were serially diluted 2-fold and added to the plates, then incubated overnight at 4°C. After washing, horseradish peroxidase-conjugated anti-mouse IgG, IgG1, or IgG2a (SouthernBiotech, Homewood, AL, USA) was added and incubated at 37°C for 1 hour. TMB substrate was used for color development. After the reaction was stopped with sulfuric acid, optical density values were read at 450 nm by a microplate reader (SpectraMax i3x; Molecular Devices, San Jose, CA, USA). Results exceeding the mean optical density of the negative control group+2 × standard deviation (SD) were considered positive. IgG titers were expressed as the highest dilution producing a positive reaction [19].

### HI assay

Functional antibodies inhibiting hemagglutination were quantified using a HI assay. Sera were treated with receptor-destroying enzyme (RDE; Denka Seiken, Tokyo, Japan) for 18 hours at 37°C and subsequently heat-inactivated at 56°C for 30 minutes. Fifty microliters of pre-treated serum were tested in twofold serial dilutions, beginning with a 1:10 dilution. The serum was mixed with an equal volume of 4 hemagglutination units of either A/Darwin/9/2021 (H3N2) virus or A/Guizhou/54/1989 (H3N2) virus and incubated for 1 hour at room temperature. After incubation, 50 μL of a 1% guinea pig red blood cell suspension was added to the mixture, and hemagglutination activity was assessed by observing the plate after 60 minutes at room temperature. The HI titer was defined as the reciprocal of the highest serum dilution showing ≥50% hemagglutination inhibition. The detection limit for the assay was a serum dilution of 1:10, and samples with undetectable HI activity were assigned a value of 10 [20].

### MN assay

The influenza virus neutralizing antibody titers were measured according to the protocol recommended by the World Health Organization (WHO). Briefly, serum samples treated with RDE were diluted 2-fold using DMEM containing 5 μg/mL TPCK-treated trypsin (Sigma-Aldrich, St. Louis, MO, USA). An equal volume of the virus, at a concentration of 100 $TCID_{50}$/50 μL, was added to the diluted serum and incubated at 37°C for 1 hour. The mixture was then added to MDCK cells ($2\times10^4$ cells per well) and incubated for 72 hours at 37°C with 5% $CO_2$. Afterwards, freshly prepared 1% guinea pig red blood cells were added, and the samples were observed 1 hour later. Neutralizing titers per milliliter of serum were calculated using the Reed and Muench method [20].

### Histopathology

On day 5 post influenza virus challenge, the mice were euthanized. The left lung lobe from each mouse was fixed in 4% paraformaldehyde and embedded in paraffin following standard histological procedures. The lung tissues were then sectioned and stained with hematoxylin and eosin. Images of the stained lung tissues were captured using a Pannoramic Desk/Midi/250/1000 slide scanner and analyzed with CaseViewer2.4 software (both from 3D Histech, Budapest, Hungary).

### Statistical analysis

Experimental data were analyzed using Prism 10.2.2 software (GraphPad, San Diego, CA, USA). Comparisons between 2 groups were performed using a t-test, while one-way analysis of variance was used for comparisons among more than 2 groups. All results are presented as mean ± SD.

Protein sequence alignment was performed using SnapGene 6.0.2 (Insightful Science, San Diego, CA, USA) with the local alignment (Smith-Waterman) algorithm.

Protein structure analysis was conducted using homology modeling in SWISS-MODEL (https://swissmodel.expasy.org). The model protein was obtained from the PDB database. Subsequently, the structures of different proteins were visualized, aligned, and analyzed using ChimeraX 1.9.0.

## RESULTS

### Generation and characterization of recombinant ferritin-HA nanoparticles

Recombinant ferritin-HA nanoparticles (**Fig. 2A**) were expressed in CHO-S cells and purified using nickel affinity chromatography. Sodium dodecyl sulfate-polyacrylamide gel electrophoresis analysis revealed a prominent band with an approximate molecular weight of 100 kDa (**Fig. 2B**), while the SEC chromatogram obtained via HPLC displayed a single major peak (**Fig. 2D**). Hemagglutination assays confirmed that the ferritin-HA protein retained its natural hemagglutinating activity (**Fig. 2B**). Dynamic light scattering analysis showed that the ferritin-HA nanoparticles predominantly measured around 40 nm in diameter (**Fig. 2C**), consistent with the TEM images (**Fig. 2E**). TEM further revealed that the ferritin-HA nanoparticles featured a bright spherical core with multiple radial spikes. These results suggest that the recombinant ferritin-HA protein successfully self-assembling into uniformly sized nanoparticles.

 https://doi.org/10.7774/cevr.2025.14.e7

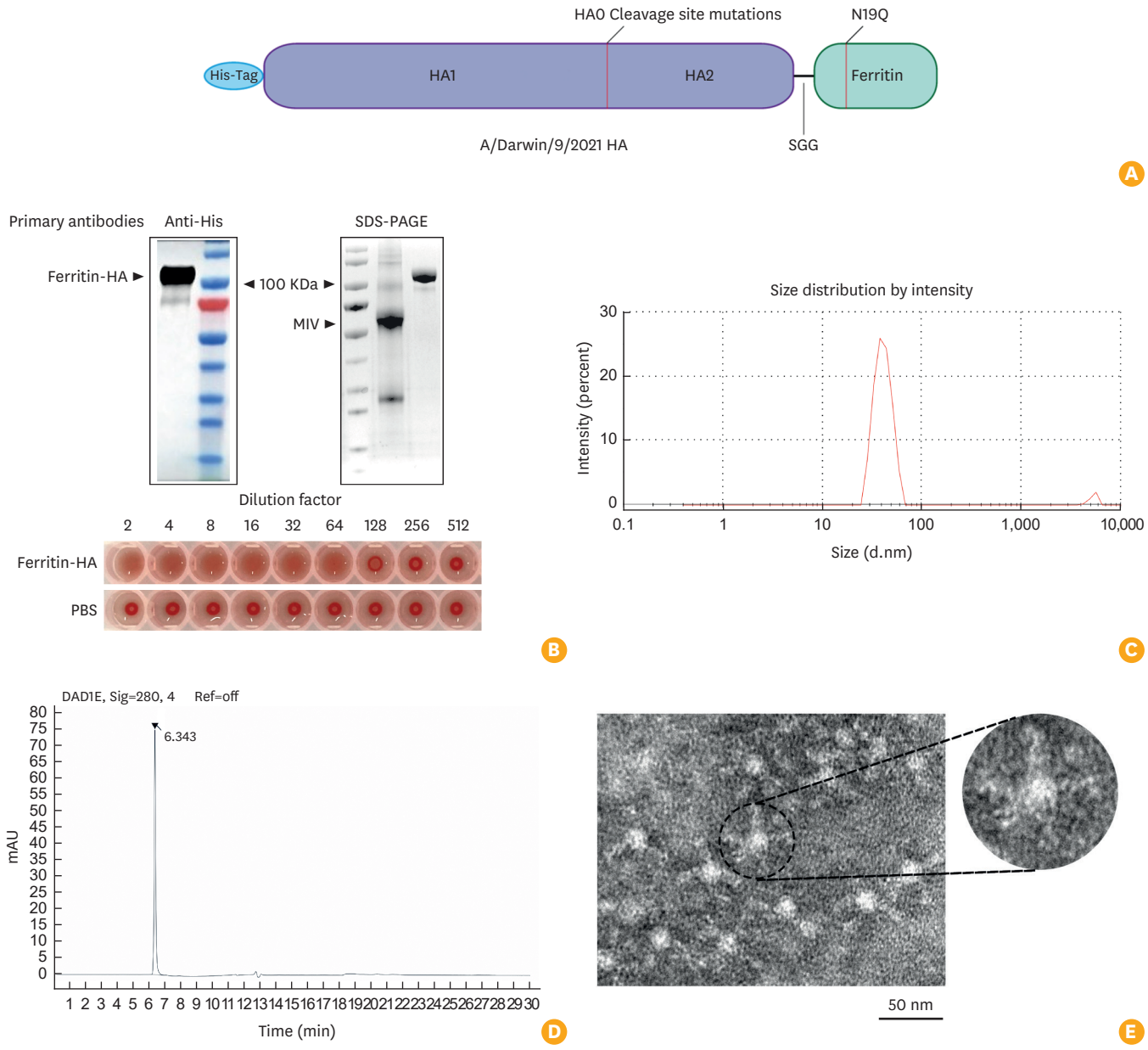


**Fig. 2.** Identification and characterization of ferritin-HA nanoparticles *in vitro*. (A) Schematic diagram of the design of ferritin-HA. (B) Western blot identification, SDS-PAGE analysis, and hemagglutination activity assay of ferritin-HA. (C) The particle size of ferritin-HA nanoparticles was around 40 nm in diameter analyzed by dynamic light scattering. (D) The purity of ferritin-HA nanoparticles was over 95% detected by High Performance Liquid Chromatography. (E) Transmission electron microscope image of ferritin-HA nanoparticles (detailed protocols for all analyses were provided in the MATERIALS AND METHODS section).
HA, hemagglutinin; SDS-PAGE, sodium dodecyl sulfate-polyacrylamide gel electrophoresis; MIV, monovalent influenza split virion vaccine; PBS, phosphate-buffered saline.

## Ferritin-HA nanoparticles enhanced antigen uptaking and maturation of DCs

To analyze the ability of ferritin-HA nanoparticles to be delivered by DCs and promote DCs maturation, we incubated fluorescently labeled ferritin-HA nanoparticles or MIV with JAWS II cells for 24 hours, the uptaking of the proteins was observed using confocal microscopy. The results showed that DCs treated with ferritin-HA nanoparticles exhibited higher fluorescence intensity compared to MIV (**Fig. 3A**). Additionally, the upregulation of CD80 molecules on the surface of DCs in the ferritin-HA group was notably higher than that in the control group (NEG) and approximately 10% higher than in the MIV group (81.25% vs. 70.04%, $p<0.0001$) (**Fig. 3B**). These findings suggest that ferritin-HA

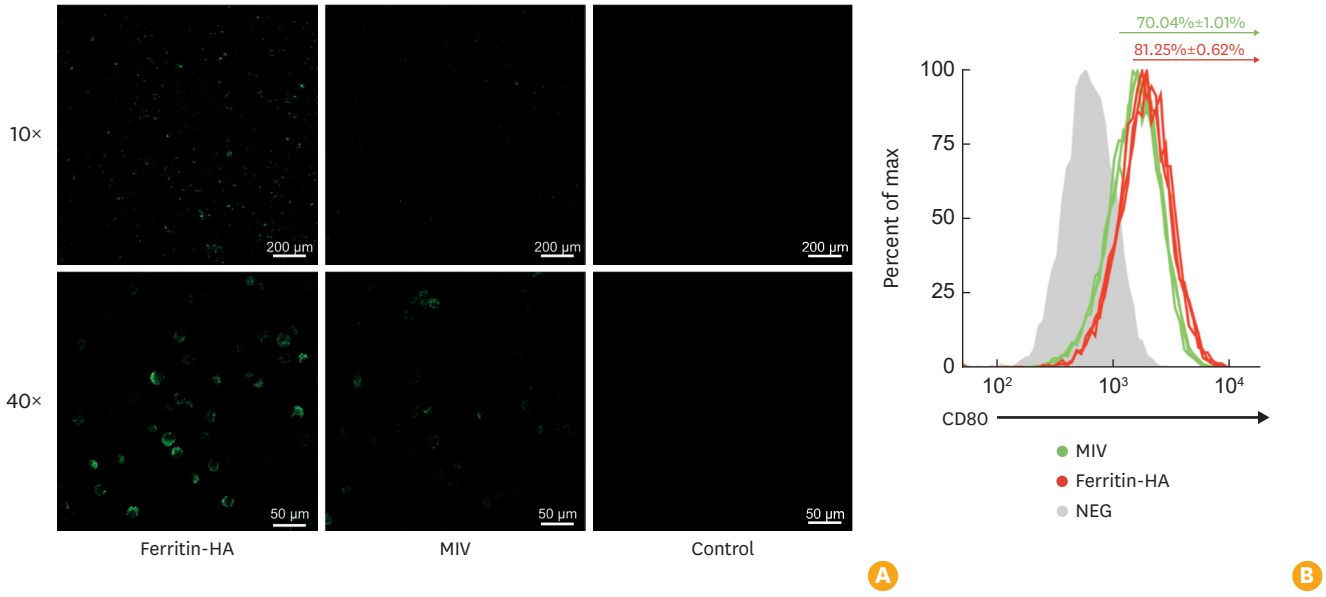


**Fig. 3.** The ferritin-HA nanoparticles effectively promoted antigen uptake and maturation of JAWS II cells. Fluorescence images (A) showing the uptake of AlexaFluor-488-labeled (green) ferritin-HA nanoparticles or MIV by JAWS II cells. The proportion of $CD80^+$ JAWS II cells (B) after 24 hours of stimulation with ferritin-HA nanoparticles or MIV.
HA, hemagglutinin; MIV, monovalent influenza split virion vaccine; NEG, control group.

nanoparticles effectively enhance antigen uptake and promote DCs maturation.

## Ferritin-HA vaccine induced robust humoral immune responses

To investigate the immunogenicity of the vaccine formulation, mice were immunized intramuscularly twice with various doses of ferritin-HA alone or in combination with $Al(OH)_3$ adjuvant. Sera were collected from the mice at 21-day intervals for further analysis.

The titers of HA specific total IgG in serum were measured by ELISA. We found that the vaccine induced IgGs reactive to MIV or trimeric HA protein, with a dose-dependency. Following intensive immunization, MIV-induced IgG levels were higher than those induced by 0.015 μg ferritin-HA (**Fig. 4A**), likely due to the presence of additional viral antigenic components in MIV. The IgG, reactive to trimeric HA protein, induced by 0.015 μg ferritin-HA alone or combined with $Al(OH)_3$ were significantly higher than those induced by MIV post boost ($p<0.0001$) (**Fig. 4B**).

IgG1 or IgG2a can indirectly reflect the bias towards Th1 or Th2 immune responses [21]. The levels of IgG1 or IgG2a showed a similar trend to that of IgG post boost. The ratio of IgG2a/IgG1 was closer to 1 in mice immunized with the ferritin-HA alone or in combination with $Al(OH)_3$ compared with MIV (**Fig. 4C**), suggesting that the ferritin-HA induced a more balanced Th1 and Th2 response.

HI antibody titers are classic indicators for evaluating the immunogenicity of influenza vaccines. All vaccinated mice elicited no less than 1:40 HI levels post prime. Following the booster vaccination, the HI titers produced by 0.015 μg ferritin-HA combined with $Al(OH)_3$ reached as high as 1:1,280, approximately five times higher than those induced by MIV ($p<0.05$) (**Fig. 4D**).

We further evaluated the MN antibody response, which is crucial for assessing the ability of antibodies to inhibit viral entry or replication. Ferritin-HA paired with $Al(OH)_3$ adjuvant induced an MN antibody titer of 1:1,778 against the A/Darwin/9/2021 (H3N2) virus, which was higher than the titer induced by 0.15 μg ferritin-HA and 0.015 μg MIV, though the difference was not statistically significant (**Fig. 4E**). We also assessed the vaccines' ability to induce cross-neutralizing antibodies. The levels of MN antibody levels induced against the A/Guizhou/54/1989 (H3N2) virus were consistent with those against the A/Darwin/9/2021 (H3N2) virus in each vaccine group. However, the MN antibody titers against A/Guizhou/54/1989 (H3N2) were significantly lower, amounting to only one-tenth of the values observed against A/Darwin/9/2021 (H3N2). Notably, ferritin-HA combined with $Al(OH)_3$ adjuvant produced significantly higher levels of cross-neutralizing antibodies than MIV ($p<0.001$) (**Fig. 4F**).

Given that B-cell proliferation and affinity maturation within the germinal center depend heavily on coordinated T-cell support, which is crucial for an efficient humoral

 https://doi.org/10.7774/cevr.2025.14.e7

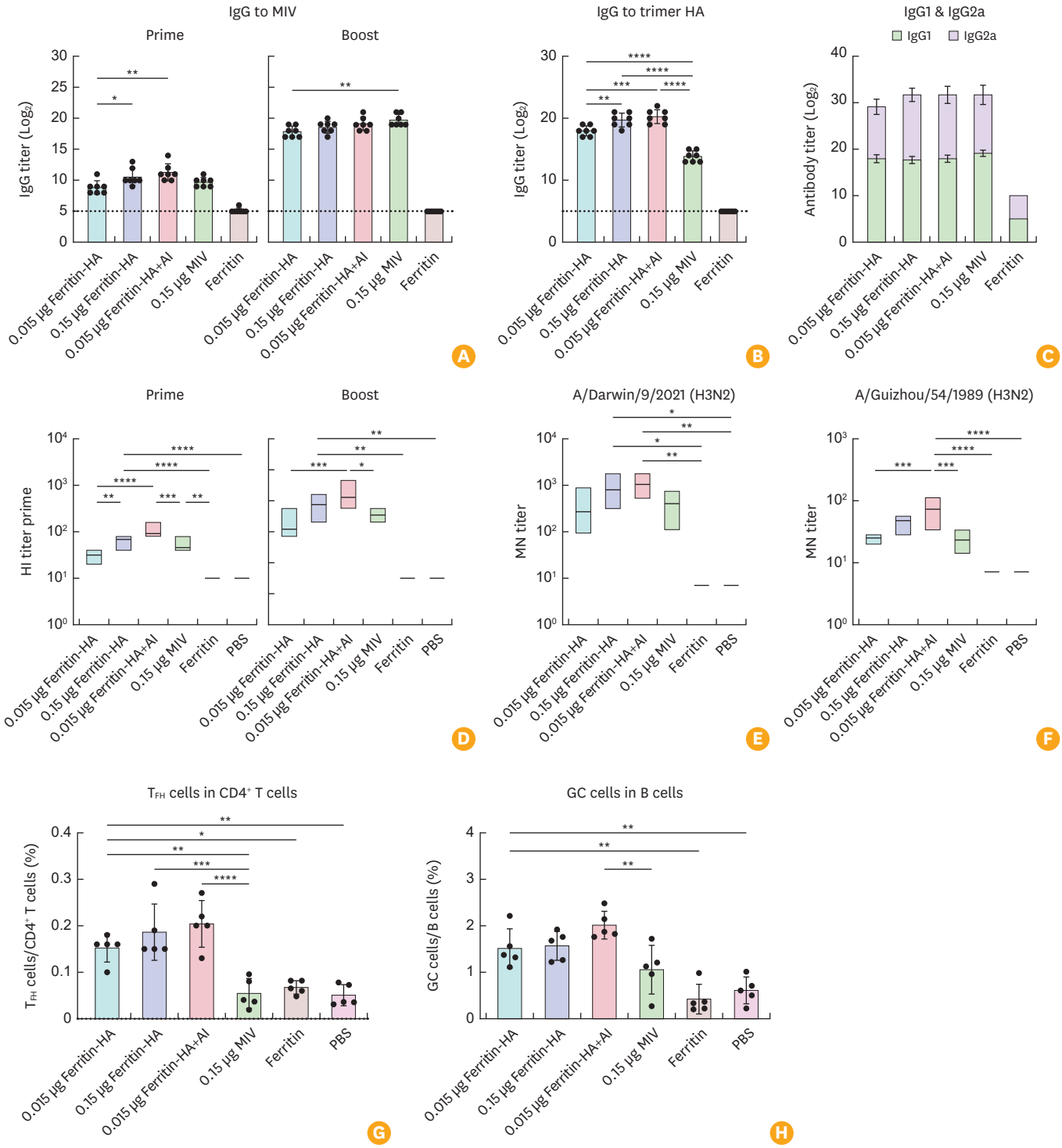


**Fig. 4.** The ferritin-HA nanoparticle vaccination elicited humoral immune responses. The MIV-specific IgG antibodies (A), trimeric HA protein-specific IgG antibodies (B), and MIV-specific IgG1 and IgG2a antibodies (C) in mice (n=7) serum were quantified by ELISA on day 21 post prime and boost immunization. (D) The HI detection against A/Darwin/9/2021 (H3N2) virus on day 21 post prime and boost immunization (n=7). (E) The MN antibody levels against A/Darwin/9/2021 (H3N2) virus or (F) A/Guizhou/54/1989 (H3N2) virus on day 21 post boost immunization. The proportions of (G) PD-1$^+$ CXCR5$^+$ $T_{FH}$ cells and (H) GL7$^+$ CD95$^+$ GC B cells in spleen of mice were analyzed by flow cytometry (n=5). Data significance was determined using one-way ANOVA.

HA, hemagglutinin; MIV, monovalent influenza split virion vaccine; IgG, immunoglobulin G; ELISA, enzyme-linked immunosorbent assay; HI, hemagglutination inhibition; $T_{FH}$, follicular helper T; GC, germinal center; ANOVA, analysis of variance; PBS, phosphate-buffered saline.

*p<0.05, **p<0.01, ***p<0.001, ****p<0.0001.

immune response[22,23], we aimed to investigate whether the ferritin-HA vaccine could further demonstrate its efficacy by enhancing the number of follicular helper T ($T_{FH}$) and germinal center (GC) B cells in the spleen. The proportion of $CXCR5^+$ $PD\text{-}1^+$ $T_{FH}$ cells activated by the 0.015 μg ferritin-HA was significantly higher than that of MIV ($p<0.01$) (**Fig. 4G**). As expected, the ferritin-HA combined with $Al(OH)_3$ also induced a remarkably higher proportion of GC B cells ($GL7^+$ and $CD95^+$) compared to the MIV ($p<0.01$) (**Fig. 4H**), implying that the ferritin-HA has a superior ability to promote GC B cells maturation.

### Protective efficacy of ferritin-HA vaccine against influenza virus challenge in mice

Studies have shown that vaccines based on the ferritin carrier exhibit enhanced cross-protection [24], and adjuvants can further amplify these effects [25]. Therefore, we further assessed whether the ferritin-HA could provide protection against the challenge of heterologous A/Guizhou/54/1989 (H3N2) virus.

All mice in each group experienced weight loss and infection symptoms post challenge. The mice in control groups (PBS, ferritin) suffered severe disease reactions and all died by day 9 (mice with weight loss greater than 25% were euthanized). Mice vaccinated with ferritin-HA plus $Al(OH)_3$ adjuvant only lost about 15% of their body weight and began to recover by day 6 (**Fig. 5A**).

Survival rates were consistent with weight change trends. Almost all groups showed varying degrees of protection against influenza virus, except for the control groups and the 0.015 μg ferritin HA group. About 20% (n=9) of the mice survived in MIV group, while the same dose of ferritin-HA provided 30% (n=9) protection. The addition of adjuvants further enhanced the protective effect, and the combined immunization of ferritin-HA and $Al(OH)_3$ provided 100% protection (n=9) (**Fig. 5B**). These results attested that the ferritin-HA, especially when used in combination with an aluminum adjuvant, significantly enhanced protection against influenza virus challenge in mice.

Timely clearance of the virus following influenza infection is crucial for recovery. We assessed the residual viral load in the lungs of mice using the $TCID_{50}$ assay and found that mice immunized with the adjuvanted ferritin-HA vaccine had significantly lower viral titers on day 5 post-challenge compared to the control group (**Fig. 5C**). Additionally, lung histopathology analysis performed on day 5 revealed that samples from the PBS control group exhibited alveolar septal thickening, mixed inflammatory cell infiltrates, diffuse perivascular necrosis, and inflammation around the bronchi and blood vessels (**Fig. 5D**). In contrast, the adjuvanted ferritin-HA group showed a marked reduction in inflammation around the bronchi, with the alveolar structure largely intact. These findings suggest that the ferritin-HA vaccine provides strong heterologous protection against influenza virus in the murine model.

## DISCUSSION

WHO annually recommends candidate strains for influenza vaccine production based on global surveillance data. However, antigenic mismatches between vaccine strains and circulating strains influenza viruses still pose a challenge to the current protective efficacy of influenza vaccines. Thus, until broad-spectrum influenza vaccines become a reality, there is an urgent need for next-generation influenza vaccines with effective designs or formulations.

In this study, we successfully developed a recombinant protein-based nanoparticle vaccine by displaying the extracellular domain of the influenza HA trimer on ferritin. The nanoparticle's self-assembling into well-defined particles highlights its feasibility as a vaccine platform. Previous studies have used HA or other trimeric structures for similar purposes, demonstrating promising immunogenicity and protective effects in different animal models [11-15,26]. Ferritin has proven to be a versatile scaffold for presenting HA trimers and forming particles that mimic viral structures, this capability to mimic virus particles and form protein trimers has been validated in several studies [26,27]. This reinforces its potential for use in next-generation influenza vaccines.

Several studies have shown that spherical nanoparticle structures such as PLGA or ferritin exhibit superior performance in promoting DC cell function and inducing influenza-neutralizing antibodies [26,28,29]. Similarly, we observed that ferritin-HA nanoparticles could promote the antigen uptake capability and maturation of DCs, and elevate the levels of induced HI and MN antibodies. Besides, Immunization with the ferritin-HA nanoparticles significantly increased the proportions of $T_{FH}$ and GC B cells in the spleen of mice compared to the MIV, which is in concordance with the studies on ferritin-based COVID-19 vaccines. This may represent a key mechanism by which ferritin nanoparticle vaccines enhance the immune response, particularly the antibody response [30].

During our study, we found that ferritin induced some level of cross-protection against a heterologous virus, and previous research has shown that HA2, when paired with ferritin, can mediate strong cross-protection [31]. Our ferritin-HA nanoparticle vaccine, which focuses on the HA trimer, may similarly induce cross-reactive antibodies

 https://doi.org/10.7774/cevr.2025.14.e7

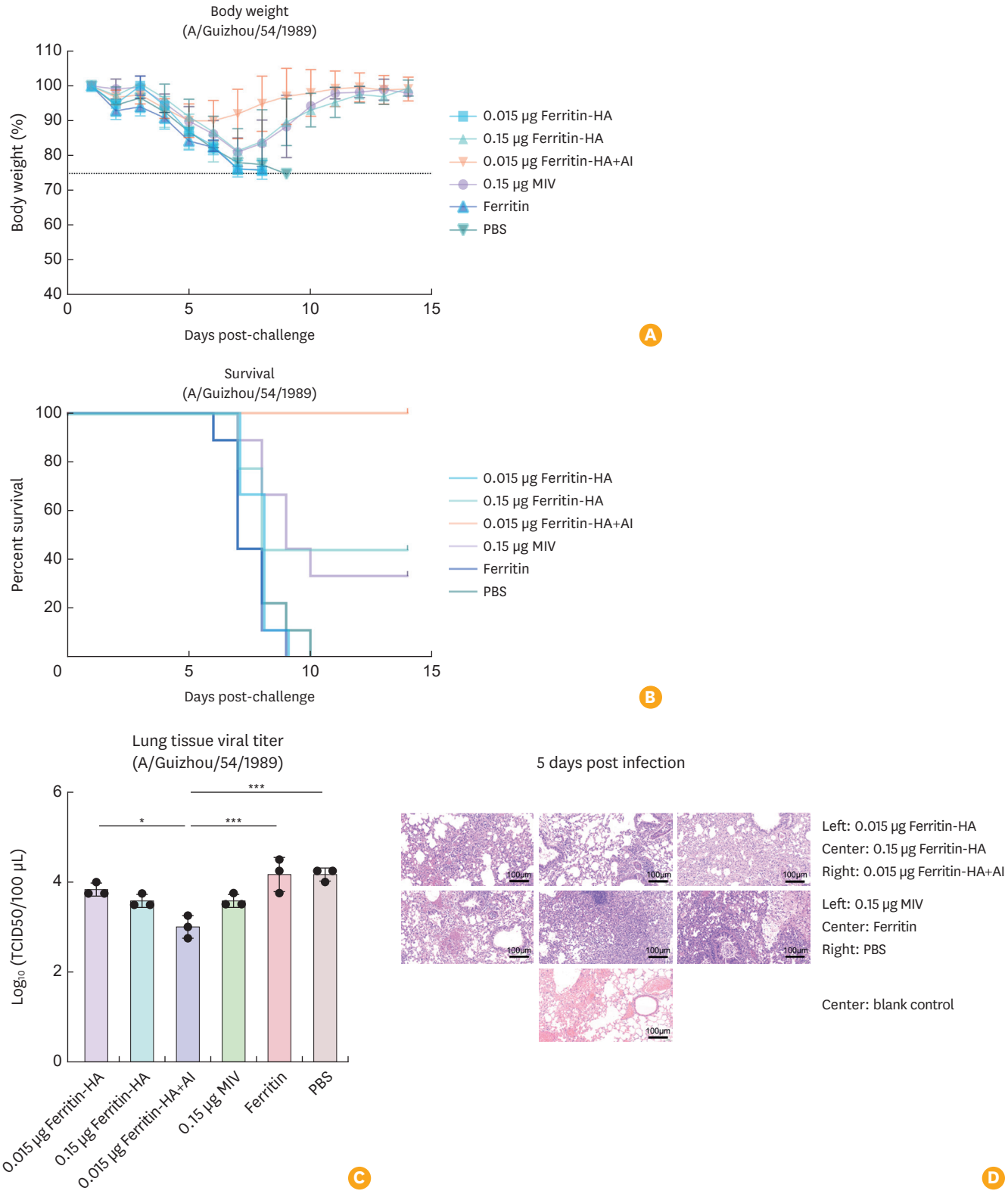


**Fig. 5.** The ferritin-HA nanoparticle vaccination protected mice from heterologous influenza virus challenge. BALB/c mice were challenged intranasally with a lethal dose (5×$LD_{50}$) of A/Guizhou/54/1989 (H3N2) influenza virus on day 28 post boost immunization. The body weight changes (A) and survival rates (B) of the mice (n=9) were monitored for 14 days. The lung viral titers (C) and hematoxylin and eosin staining of the lung was performed on day 5 post-challenge (D). Data significance was quantified using one-way ANOVA.
HA, hemagglutinin; ANOVA, analysis of variance; MIV, monovalent influenza split virion vaccine; PBS, phosphate-buffered saline; $TCID_{50}$, 50% tissue culture infectious dose.
*p<0.05, ***p<0.001.

targeting the conserved HA2 fusion domain. This domain plays a crucial role in viral membrane fusion and is a major target for broad-spectrum neutralizing antibodies. The structural stability provided by ferritin ensures proper presentation of the HA2 epitope, potentially inducing HA2-specific antibodies that contribute to cross-protection against different influenza strains [27]. This hypothesis aligns with the observed cross-protection conferred by our vaccine in mice.

To explore the reasons for the heterologous protection induced by the ferritin-HA, a comparison of the HA1 amino acid sequences of A/Guizhou/54/1989 (H3N2) and A/Darwin/9/2021 (H3N2) strains revealed approximately 91% homology (**Fig. 6A**). The K189Q mutation involves the 190 helix of the receptor-binding site (RBS), and the K156I mutation is located at the periphery of the receptor-binding domain (**Fig. 6B**) [32,33]. Additionally, other amino acid sites in the RBS region exhibited varying degrees of mutation, suggesting that neutralizing antibodies might target the more conserved stem region of HA antigen. It has been shown that ferritin-based trimeric HÀ has a spatial structure closer to the native fold of the real virus than trimeric HA based on foldon. This structural similarity could more effectively mimic viral antigen epitopes, enhance immunogenicity and increase the production of HA antibodies, thereby enhancing the protective efficacy of the vaccine [27] and suggests that future studies should further investigate the role of HA2-targeting antibodies in this protective mechanism.

In conclusion, this study demonstrates that our self-assembling ferritin-HA nanoparticle vaccine, displaying the extracellular domain of the HA from H3N2 influenza virus, holds great potential as a next-generation influenza vaccine candidate. The ferritin-HA nanoparticles significantly enhanced humoral immune responses, including elevated levels of IgG, HI, and MN antibodies, compared to traditional split virion influenza vaccines. Furthermore, the vaccine promoted stronger antigen uptake and maturation of DCs, which are crucial for an effective immune response. When used in conjunction with aluminum adjuvant, it provided complete protection against a lethal challenge from heterologous influenza strains in mice. These results suggest that the ferritin-HA nanoparticle platform is a promising strategy for the development of a more effective or broad-spectrum influenza vaccine.


**Fig. 6.** Heterologous HA sequence alignment and structural prediction analysis. (A) Alignment of HA1 sequences from A/Darwin/9/2021 and A/Guizhou/54/1989 strains, performed using SnapGene 6.0.2 with the Smith-Waterman local alignment algorithm. Amino acid differences are marked with "X," and similar mutations with "+" for clarity. (B) HA trimers structure in prediction (PDB ID of the model structure: 6n08), chain b & chain c are showed in pink and orange red. HA of A/Guizhou/54/1989 is showed in yellow while A/Darwin/9/2021 is in cornflower blue. Partial details are zoomed in where certain critical mutations are displayed.
HA, hemagglutinin.

(continued to the next page)

 https://doi.org/10.7774/cevr.2025.14.e7

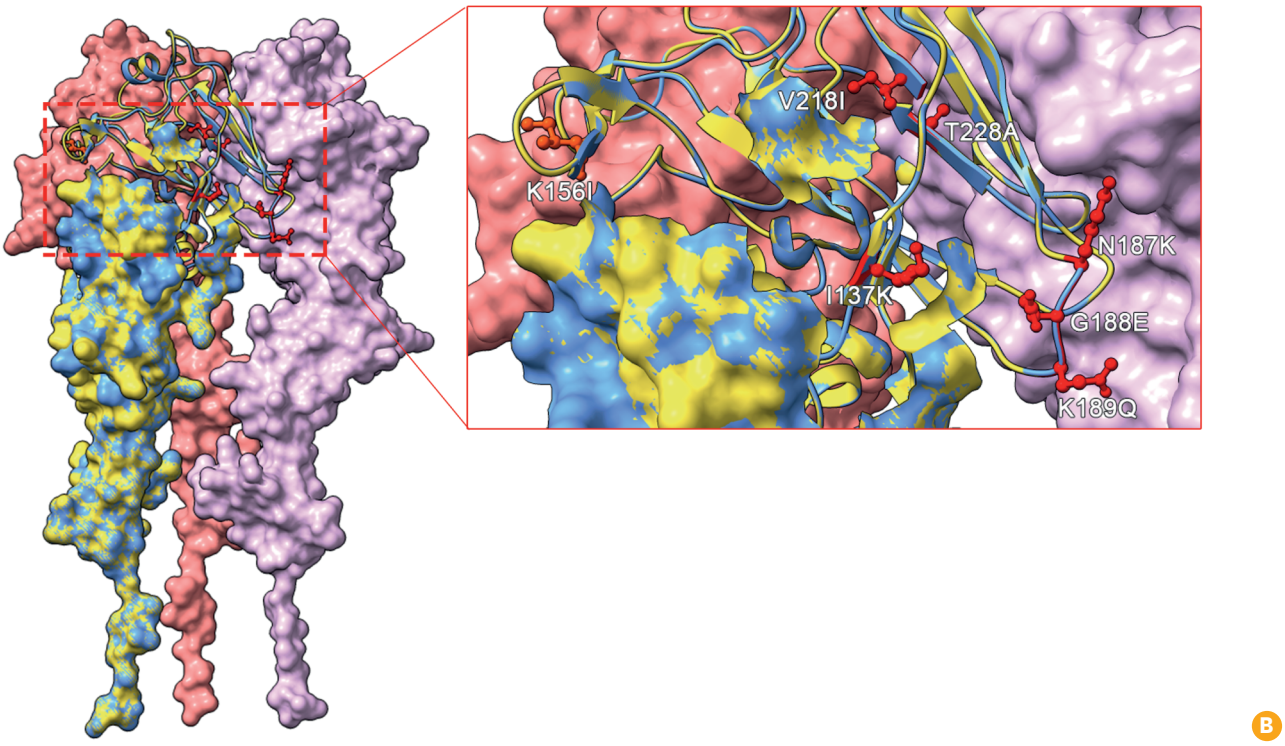


**Fig. 6.** (Continued) Heterologous HA sequence alignment and structural prediction analysis. (A) Alignment of HA1 sequences from A/Darwin/9/2021 and A/Guizhou/54/1989 strains, performed using SnapGene 6.0.2 with the Smith-Waterman local alignment algorithm. Amino acid differences are marked with "X," and similar mutations with "+" for clarity. (B) HA trimers structure in prediction (PDB ID of the model structure: 6n08), chain b & chain c are showed in pink and orange red. HA of A/Guizhou/54/1989 is showed in yellow while A/Darwin/9/2021 is in cornflower blue. Partial details are zoomed in where certain critical mutations are displayed.
HA, hemagglutinin.

ORCID iDs
Xu Wang
https://orcid.org/0009-0004-2937-8186
Ziyao Qin
https://orcid.org/0000-0002-4329-4956
Min Zhang
https://orcid.org/0009-0000-0278-6607
Baoyuan Shang
https://orcid.org/0000-0003-4545-9061
Zhilei Li
https://orcid.org/0009-0005-9137-0625
Meiyi Zhao
https://orcid.org/0009-0002-7360-8968
Qing Tang
https://orcid.org/0009-0005-8307-6266
Qi Tang
https://orcid.org/0009-0005-4515-9204
Jian Luo
https://orcid.org/0000-0003-4685-9008

Funding
This work was supported by the National Key Research and Development Program of China (2023YFC2606000).

Conflict of Interest
No potential conflict of interest relevant to this article was reported.

## REFERENCES

1. Reed C, Angulo FJ, Swerdlow DL, et al. Estimates of the prevalence of pandemic (H1N1) 2009, United States, April-July 2009. Emerg Infect Dis 2009;15:2004-7. PUBMED | CROSSREF
2. Vemula SV, Zhao J, Liu J, Wang X, Biswas S, Hewlett I. Current approaches for diagnosis of influenza virus infections in humans. Viruses 2016;8:96. PUBMED | CROSSREF
3. Word Health Organization (WHO). Up to 650 000 people die of respiratory diseases linked to seasonal flu each year. Geneva: WHO; [cited 2018 Dec 13]. Available from: https://www.who.int/zh/news/item/14-12-2017-up-to-650-000-people-die-of-respiratory-diseases-linked-to-seasonal-flu-each-year.
4. Centers for Disease Control and Prevention (CDC). Images of Influenza Viruses 2019. Atlanta, GA: CDC; [cited 2023 Jan 4]. Available from: https://www.cdc.gov/flu-resources/php/resources/.

5. Robertson JS, Bootman JS, Newman R, et al. Structural changes in the haemagglutinin which accompany egg adaptation of an influenza A(H1N1) virus. Virology 1987;160:31-7. PUBMED | CROSSREF
6. Katz JM, Wang M, Webster RG. Direct sequencing of the HA gene of influenza (H3N2) virus in original clinical samples reveals sequence identity with mammalian cell-grown virus. J Virol 1990;64:1808-11. PUBMED | CROSSREF
7. Katz JM, Webster RG. Amino acid sequence identity between the HA1 of influenza A (H3N2) viruses grown in mammalian and primary chick kidney cells. J Gen Virol 1992;73:1159-65. PUBMED | CROSSREF
8. Puig-Barberà J, Tamames-Gómez S, Plans-Rubio P, Eiros-Bouza JM. Relative effectiveness of cell-cultured versus egg-based seasonal influenza vaccines in preventing influenza-related outcomes in subjects 18 years old or older: a systematic review and meta-analysis. Int J Environ Res Public Health 2022;19:818. PUBMED | CROSSREF
9. Barr IG, Donis RO, Katz JM, et al. Cell culture-derived influenza vaccines in the severe 2017-2018 epidemic season: a step towards improved influenza vaccine effectiveness. NPJ Vaccines 2018;3:44. PUBMED | CROSSREF
10. Truffi M, Fiandra L, Sorrentino L, Monieri M, Corsi F, Mazzucchelli S. Ferritin nanocages: A biological platform for drug delivery, imaging and theranostics in cancer. Pharmacol Res 2016;107:57-65. PUBMED | CROSSREF
11. Kanekiyo M, Bu W, Joyce MG, et al. Rational design of an Epstein-Barr virus vaccine targeting the receptor-binding site. Cell 2015;162:1090-100. PUBMED | CROSSREF
12. Olshefsky A, Richardson C, Pun SH, King NP. Engineering self-assembling protein nanoparticles for therapeutic delivery. Bioconjug Chem 2022;33:2018-34. PUBMED | CROSSREF
13. Swanson KA, Rainho-Tomko JN, Williams ZP, et al. A respiratory syncytial virus (RSV) F protein nanoparticle vaccine focuses antibody responses to a conserved neutralization domain. Sci Immunol 2020;5:eaba6466. PUBMED | CROSSREF
14. Powell AE, Zhang K, Sanyal M, et al. A single immunization with spike-functionalized ferritin vaccines elicits neutralizing antibody responses against SARS-CoV-2 in mice. ACS Cent Sci 2021;7:183-99. PUBMED | CROSSREF
15. Joyce MG, Chen WH, Sankhala RS, et al. SARS-CoV-2 ferritin nanoparticle vaccines elicit broad SARS coronavirus immunogenicity. Cell Reports 2021;37:110143. PUBMED | CROSSREF
16. Widge AT, Hofstetter AR, Houser KV, et al. An influenza hemagglutinin stem nanoparticle vaccine induces cross-group 1 neutralizing antibodies in healthy adults. Sci Transl Med 2023;15:eade4790. PUBMED | CROSSREF
17. Andrews SF, Cominsky LY, Shimberg GD, et al. An influenza H1 hemagglutinin stem-only immunogen elicits a broadly cross-reactive B cell response in humans. Sci Transl Med 2023;15:eade4976. PUBMED | CROSSREF
18. Keskin DB, Anandappa AJ, Sun J, et al. Neoantigen vaccine generates intratumoral T cell responses in phase Ib glioblastoma trial. Nature 2019;565:234-9. PUBMED | CROSSREF
19. Xiong F, Zhang C, Shang B, et al. An mRNA-based broad-spectrum vaccine candidate confers cross-protection against heterosubtypic influenza A viruses. Emerg Microbes Infect 2023;12:2256422. PUBMED | CROSSREF
20. Gao F, Liu X, Dang Y, et al. AddaVax-adjuvanted H5N8 inactivated vaccine induces robust humoral immune response against different clades of H5 viruses. Vaccines (Basel) 2022;10:1683. PUBMED | CROSSREF
21. Hochreiter R, Ferreira F, Thalhamer J, Hammerl P. TH1-promoting DNA immunization against allergens modulates the ratio of IgG1/IgG2a but does not affect the anaphylactic potential of IgG1 antibodies: no evidence for the synthesis of nonanaphylactic IgG1. J Allergy Clin Immunol 2003;112:579-84. PUBMED | CROSSREF
22. Baumjohann D, Preite S, Reboldi A, et al. Persistent antigen and germinal center B cells sustain T follicular helper cell responses and phenotype. Immunity 2013;38:596-605. PUBMED | CROSSREF
23. Shulman Z, Gitlin AD, Targ S, et al. T follicular helper cell dynamics in germinal centers. Science 2013;341:673-7. PUBMED | CROSSREF
24. Rodrigues MQ, Alves PM, Roldão A. Functionalizing ferritin nanoparticles for vaccine development. Pharmaceutics 2021;13:1621. PUBMED | CROSSREF
25. Li Z, Zhao Y, Li Y, Chen X. Adjuvantation of influenza vaccines to induce cross-protective immunity. Vaccines (Basel) 2021;9:75. PUBMED | CROSSREF
26. Kanekiyo M, Wei CJ, Yassine HM, et al. Self-assembling influenza nanoparticle vaccines elicit broadly neutralizing H1N1 antibodies. Nature 2013;499:102-6. PUBMED | CROSSREF
27. Yassine HM, Boyington JC, McTamney PM, et al. Hemagglutinin-stem nanoparticles generate heterosubtypic influenza protection. Nat Med 2015;21:1065-70. PUBMED | CROSSREF
28. Petrizzo A, Conte C, Tagliamonte M, et al. Functional characterization of biodegradable nanoparticles as antigen delivery system. J Exp Clin Cancer Res 2015;34:114. PUBMED | CROSSREF
29. Han JA, Kang YJ, Shin C, et al. Ferritin protein cage nanoparticles as versatile antigen delivery nanoplatforms for dendritic cell (DC)-based vaccine development. Nanomedicine 2014;10:561-9. PUBMED | CROSSREF
30. Ma X, Zou F, Yu F, et al. Nanoparticle vaccines based on the receptor binding domain (RBD) and heptad repeat (HR) of SARS-CoV-2 elicit robust protective immune responses. Immunity 2020;53:1315-1330.e9. PUBMED | CROSSREF
31. Moin SM, Boyington JC, Boyoglu-Barnum S, et al. Co-immunization with hemagglutinin stem immunogens elicits cross-group neutralizing antibodies and broad protection against influenza A viruses. Immunity 2022;55:2405-2418.e7. PUBMED | CROSSREF
32. Quan L, Ji C, Ding X, et al. Cluster-transition determining sites underlying the antigenic evolution of seasonal influenza viruses. Mol Biol Evol 2019;36:1172-86. PUBMED | CROSSREF
33. Yang H, Carney PJ, Chang JC, Guo Z, Villanueva JM, Stevens J. Structure and receptor binding preferences of recombinant human A(H3N2) virus hemagglutinins. Virology 2015;477:18-31. PUBMED | CROSSREF